Journal Pre-proofs

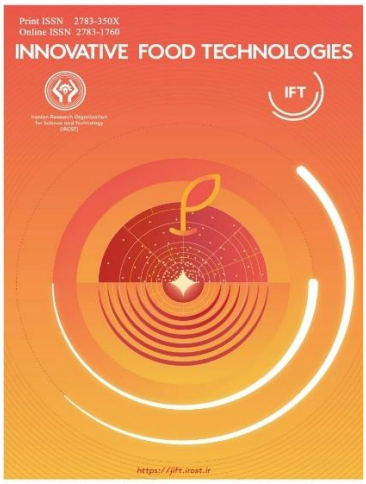

Optimised Spray-Dried Momordica charantia Microencapsulation with Techno-Economic and Market-Diffusion Analysis for Functional Beverages

Amiesha Nur Shaheerah Mazlan, Siti Nursyazweena Zul-kharnain, Mohamad Syafiq Abdul Wahab, Siti Hawa Mat Yaman, Rasyidah Alrozi, Mohd Othman Halim, Mohamed Syazwan Osman

DOI: https://doi.org/10.22104/ift.2026.8285.2297

To appear in: Innovative Food Technologies (IFT)

Received Date: 25 May 2026
Revised Date: 24 August 2026
Accepted Date: 26 August 2026

Please cite this article as: Amiesha Nur Shaheerah Mazlan, Siti Nursyazweena Zul-kharnain, Mohamad Syafiq Abdul Wahab, Siti Hawa Mat Yaman, Rasyidah Alrozi, Mohd Othman Halim, Mohamed Syazwan Osman, Optimised Spray-Dried Momordica charantia Microencapsulation with Techno-Economic and Market-Diffusion Analysis for Functional Beverages, *Innovative Food Technologies (2026)*, doi: https://doi.org/10.22104/ift.2026.8285.2297

Optimised Spray-Dried *Momordica charantia* Microencapsulation with Techno-Economic and Market-Diffusion Analysis for Functional Beverages

Amiesha Nur Shaheerah Mazlan[1], Siti Nursyazweena Zul-kharnain[1], Mohamad Syafiq Abdul Wahab[1,2], Siti Hawa Mat Yaman[1,2] Rasyidah Alrozi[1], Mohd Othman Halim[2], Mohamed Syazwan Osman[1,*]

[1] EMZI–UiTM Nanoparticles, Colloids & Interface Industrial Research Laboratory (NANO-CORE), Faculty of Chemical Engineering, Universiti Teknologi MARA, Cawangan Pulau Pinang, Kampus Permatang Pauh, 13500 Penang, Malaysia
[2] EMZI Holding Sdn Bhd, EMZI HQ, Menara Kompleks SP Plaza, Jalan Ibrahim, 08000 Sungai Petani, Kedah, Malaysia
* Corresponding author. Email: syazwan.osman@uitm.edu.my

Abstract
Spray-dried microencapsulation stabilises heat-sensitive plant bioactives into shelf-stable, beverage-compatible powders, yet the commercial viability of optimised laboratory-scale processes is rarely evaluated. *Momordica charantia* L. (bitter melon), whose phenolics, flavonoids, and triterpenes exert hypoglycaemic and antioxidant activities, remains a well-characterised but under-commercialised candidate for functional beverage applications. *M. charantia* extract was optimised via aqueous maceration and spray-drying microencapsulation using Response Surface Methodology with a two-level full factorial design (RSM–FFD) across four factors: extraction time (30–120 min), carrier type (maltodextrin or gum arabic), carrier loading (10–15% w/v of wall material relative to the total feed solution), and inlet air temperature (140–160 °C), with DPPH radical scavenging activity and powder yield as dual responses. Both models were significant (DPPH model: $R^2 = 0.9071$, Adjusted $R^2 = 0.7214$, Predicted $R^2 = 0.0489$, $p \leq 0.047$; powder yield model: $R^2 = 0.9786$, Adjusted $R^2 = 0.9541$, Predicted $R^2 = 0.8882$, $p < 0.0001$). At the desirability-function optimum (117.67 min, 15% maltodextrin, 140 °C), the encapsulate exhibited DPPH scavenging of 53.58 ± 1.24%, powder yield of 9.00 ± 0.45%, total phenolic content of 3.07×10^{-4} g GAE/g extract, total flavonoid content of 6.99×10^{-4} g QE/g extract, moisture content of 2.04%, and near-spherical particle morphology. A mass-balance-grounded techno-economic analysis, reflecting scale economies from laboratory to pilot production, returned unit costs of MYR 3.66/g (USD 0.78/g) at laboratory scale and MYR 1.14/g (USD 0.24/g) at pilot scale, a 3.2-fold reduction, with break-even achieved below 0.8 kg/month at MYR 8.00/g. A Gompertz diffusion model projected cumulative market revenues of MYR 0.59 to 1.67 million at year 5 within the Malaysian functional food market. By coupling process optimisation with techno-economic and market-adoption analysis, this work provides a scenario-based foundation for evaluating the commercial scale-up of *M. charantia* microencapsulate, aligned with SDG 3 (Good Health and Well-being).
Keywords: *Momordica charantia*; spray-drying microencapsulation; response surface methodology; techno-economic analysis; Gompertz diffusion model; functional beverages

1. Introduction

Type 2 *Diabetes mellitus* (T2DM) accounts for more than 90% of the 537 million adult diabetes cases worldwide and is projected to reach 783 million cases by 2045 (American Diabetes Association, 2023; International Diabetes Federation, 2021). In Malaysia, the National Health and Morbidity Survey reported a 2019 prevalence of 18.3% — approximately 3.9 million adults — with direct medical costs estimated at MYR 2.4–3.1 billion annually (Institute for Public Health, 2019; Ministry of Health Malaysia, 2020). This sustained epidemiological and economic burden has driven persistent interest in complementary

glycaemic regulators derived from food-grade plant bioactives that can be delivered through everyday consumer formats such as functional beverages (Mirmiran, 2014; Zahoor et al., 2024).

Momordica charantia L. (Cucurbitaceae), commonly known as bitter melon, is among the most extensively studied medicinal plants in this context. The fruit is rich in polypeptide-p (an insulin-like peptide), charantin (a steroidal saponin), vicine, momordicin, cucurbitacins, triterpenes, alkaloids, phenolic acids, and flavonoids, which collectively lower blood glucose through insulin-mimetic action, inhibition of α-glucosidase and α-amylase, enhanced peripheral glucose uptake, and attenuation of oxidative stress (Fig. 1) (Başar Altinterim, 2012; Caro-Ordieres et al., 2020; Jia et al., 2017; Zahoor et al., 2024). Direct incorporation of crude *M. charantia* extracts into food systems is nonetheless constrained by chemical instability under heat, light, oxygen, and acidic pH; poor aqueous solubility; pronounced inherent bitterness; and rapid gastrointestinal degradation (Arenas-Jal et al., 2020). Spray-drying microencapsulation addresses these constraints by entrapping bioactives within a food-grade polymeric matrix to produce free-flowing, shelf-stable powders with improved physicochemical stability, controlled release, and broad food-matrix compatibility (Arenas-Jal et al., 2020; Goyal et al., 2020; Toprakçı et al., 2024). Encapsulation performance is critically dependent on carrier type and concentration, inlet drying temperature, and the quality of the feed extract, which is itself dictated by the preceding extraction step (Mohammed et al., 2017; Tao et al., 2024). For *M. charantia*, extraction period in particular exerts a direct influence on encapsulation performance, since the study from, reviewed that the duration of extraction determines the concentration of phytochemicals recovered into the feed extract prior to spray drying (Malik et al., 2019). Inlet drying temperatures are similarly critical, since both excessively high and low drying temperatures can compromise the physical and chemical properties of the resulting encapsulated powder, making inlet drying temperature optimisation essential to product quality (Tan et al., 2015). Response Surface Methodology using a two-level full factorial design (RSM–FFD) provides a statistically rigorous and resource-efficient framework for the simultaneous optimisation of multiple correlated factors (Bezerra et al., 2008; Myers et al., 2016), and the framework has been successfully applied to a range of plant-bioactive extraction and food-formulation problems, including flavonoid recovery from *Moringa oleifera* (Fadil et al., 2025), antioxidant and yield optimisation from *Centella asiatica* leaves (Mohd Sabry et al., 2024), and the formulation of edible-bird-nest-based instant soup (Ismail et al., 2022).

However, RSM-FFD optimisation of *M. charantia* spray-dried microencapsulation specifically remains comparatively underexplored, and where it has been applied, studies have not extended beyond process characterisation to economic evaluation. This gap likely reflects the added complexity of the *M. charantia* system relative to the plant matrices bioactive are simultaneously heat, light, and pH labile, and the extract's pronounced inherent bitterness imposes formulation constraints not encountered with less unstable or more neutral-tasting matrices, which may deter the systematic multi-factor optimisation needed before economic feasibility can even be assessed. Studies routinely report optimised conditions and well-characterised encapsulate quality, yet rarely address whether the optimised process is economically viable at the scales relevant to commercial production. The bridge from a fully-optimised laboratory protocol to a quantitative market-adoption forecast — necessary to translate laboratory innovation into actual product on the shelf — remains, to the best of our knowledge, uncrossed in spray-dried plant-bioactive encapsulation, and is the central motivation of the present work.

It is the purpose of this work to couple RSM–FFD process optimisation with mass-balance-grounded techno-economic analysis (TEA) and a modified Gompertz market diffusion model, taking the spray-dried microencapsulation of *M. charantia* extract as a representative model system. Specifically, we (i) optimise the coupled extraction–spray-drying conditions across four factors and two responses; (ii) characterise the physicochemical and phytochemical properties of the optimised encapsulate; (iii) conduct a mass-balance-grounded TEA at both laboratory and projected pilot scale; and (iv) project the commercial adoption trajectory of the encapsulated ingredient within the Malaysian functional food market. We anticipate that this coupled analytical framework will allow the design of plant-bioactive encapsulation processes to be guided not by laboratory yield alone but by quantitative cost and market trajectories from the outset.

2. Materials and Methods

2.1. Plant material preparation

Fresh *M. charantia* fruits (Fig. 2) were procured from Pekan Bukit Mertajam Wet Market (Penang, Malaysia). No ethical approval was required as *M. charantia* is a common food crop. The fruits were washed, deseeded, and sliced to a uniform thickness of 3–5 mm. The slices were oven-dried using a forced air circulation oven (Memmert, Germany) at 50 °C to constant mass change of <0.1% of the total mass of the specimen (24–48 h) — a temperature chosen to minimise the thermal degradation of heat-labile phenolics (Kozłowska & Gruczyńska, 2018) — then pulverised and passed through a 0.5 mm aperture mesh sieve (ISO 3310-1). The resulting powder was vacuum-sealed in amber glass bottles and stored at −20 °C until use.

2.2. Experimental design: RSM two-level full factorial design (RSM–FFD)

The process optimisation was conducted by RSM using a two-level full factorial design (2^4, 16 runs) implemented in Design Expert® (v7.1.6, Stat-Ease Inc., USA) although more recent releases (v12-v13) offer expanded diagnostic and visualisation features, the core statistical algorithms underlying factorial design generation, first-order polynomial model fitting with two-way interactions, and ANOVA-based model evaluation are unchanged across versions, and v7.1.6 remains widely used and accepted in the contemporary RSM literature for process optimisation studies. Four independent variables were selected: extraction time (A: 30–120 min), carrier type (B: gum arabic vs. maltodextrin), carrier loading (C: 10–15% w/v), and inlet air temperature (D: 140–160 °C), each investigated at two levels (low/high) without centre or axial points. The design generated 16 experimental runs (Table 1), with DPPH scavenging activity (%) and powder yield (%) as the response variables. A first-order polynomial model with two-way interaction terms, of the form $Y = \beta_0 + \Sigma\beta_i x_i + \Sigma\Sigma\beta_{ij} x_i x_j + \varepsilon$, was fitted to each response by ordinary least-squares regression (Bezerra et al., 2008; Myers et al., 2016); the Box–Cox diagnostic indicated $\lambda \approx 1$ for both responses, so no data transformation was required. As this two-level factorial design does not include centre or axial points, it cannot estimate quadratic (curvature) terms; this constraint and its implications for the design's predictive scope are discussed in Sections 3.1 and 3.9. Model adequacy was evaluated by analysis of variance (ANOVA), R^2, adjusted R^2, predicted R^2, adequate precision (a signal-to-noise ratio, with values greater than 4 indicating an adequate signal for the model to navigate the design space), and coefficient of variation (CV% with values below 10% indicating good model reproducibility) (Yousafzai et al., 2026).

2.3. Extraction of *M. charantia* bioactives

Aqueous maceration was performed following Goyal et al. (2020) with minor modifications, and the protocol is conceptually consistent with the RSM-guided aqueous extraction approach used in related plant-bioactive systems (Fadil et al., 2025; Mohd Sabry et al., 2024). Briefly, 10 g of dried *M. charantia* powder was combined with 100 mL of distilled water (1:10 w/v) and extracted in a thermostatic water bath at 60 °C with magnetic agitation (150 rpm) for the prescribed period. The slurry was centrifuged (KUBOTA 4200, Japan) at 6,000 rpm for 20 min; the supernatant was vacuum-filtered through Whatman No. 1 filter paper with 20-25 µm nominal pore size (NICE ® Filter Paper Grade 101), and the marc was pressed to recover residual extract.

2.4. Preparation of spray-drying feed solution

Maltodextrin (DE 10–12; Sigma-Aldrich, USA) or gum arabic (food grade; Sigma-Aldrich, USA) was dissolved in the clarified extract at the prescribed loading. The mixture was homogenised at 3,000 rpm for 6 min and subsequently subjected to ultrasonic bath (50 W, 40 kHz, 10 min) to ensure homogeneity and facilitate uniform atomisation. (Cilek et al., 2012). No active cooling was applied during sonification; however, the indirect bath configuration, in which the sample beaker is immersed in the bath water rather than in direct contact with the probe. This distributes energy over a larger volume and reduce localised heating relative to probe sonification at an equivalent output. As a result, the risk of thermal degradation to heat-sensitive bioactive during the 10 minutes treatment was limited.

2.5. Spray drying

The feed solutions were spray-dried using a SD-2L Spray dryer (Zhengzhou Machine, China; stainless-steel two-fluid nozzle, 0.75 mm diameter per manufacturer specification). Fixed parameters

were: feed flow rate 9 mL/min (30% pump setting); atomising airflow 100% (manufacturer-rated maximum drying/atomising air volume of 105 m³/h at this setting); aspirator 100%; cleaning-pin cycle 4 s. Inlet temperature was set per experimental run (140 or 160°C); the outlet temperature was not independently controlled and varied passively ranged from 80-90°C as a function of inlet temperature and carrier type, consistent with their differing thermal and viscosity properties. Powders were collected from the cyclone separator, weighed, and stored in sealed amber vials with silica-gel desiccant at 4 °C. The full process flow from raw material to optimised encapsulate is summarised in Fig. 3.

2.6. Analytical methods

2.6.1. Powder yield

Yield (%) was calculated as the mass of collected powder divided by the mass of total dissolved solids in the feed, expressed as a percentage (Toprakçı et al., 2024). Total dissolved solids comprised the carrier material plus the aqueous extract solubles.

2.6.2. DPPH radical scavenging activity

DPPH scavenging activity was selected as a functional antioxidant response because M. charantia contains phenolic and flavonoid compounds associated with antioxidant activity, and the assay provides a rapid measure of the overall radical-scavenging capacity of the extract and encapsulate. Although DPPH is non-specific and does not directly quantify individual bioactive such as charantin, it was considered suitable for screening the antioxidant response during process optimisation. TPC and TFC were subsequently determined for the optimised encapsulate to further characterise its phytochemical content. The DPPH assay was adapted from Brand-Williams et al. (1995). A DPPH stock solution (0.4 mg/mL in 95% ethanol) was mixed with dissolved powder extract (1 g/30 mL deionised water) and incubated for 30 min at room temperature (approximately 25°C) in the dark; absorbance was measured at 517 nm. Antioxidant capacity was expressed as mg ascorbic acid equivalent (AAE)/g extract from a calibration curve ($R^2 = 0.9938$). DPPH scavenging activity (%) was calculated as $[(A_{blank} - A_{sample})/A_{blank}] \times 100$, where A_blank is the absorbance of the DPPH stock solution mixed with alcohol as the solvent (ethanol) in place of the extract, prepared and incubated under identical conditions, and A_sample is the absorbance of the DPPH-extract mixture.

2.6.3. Total phenolic content (TPC)

TPC was determined by the Folin–Ciocalteu method (Singleton & Rossi, 1965) using a gallic acid calibration series (0.01–0.05 mg/mL; $R^2 = 0.9766$) and expressed as mg gallic acid equivalent (GAE)/g extract (absorbance at 765 nm, 90 min dark incubation).

2.6.4. Total flavonoid content (TFC)

TFC was quantified by the aluminium chloride colorimetric method (Chang et al., 2002) using a quercetin calibration series (10–30 µg/mL; $R^2 = 0.9868$) and expressed as mg quercetin equivalent (QE)/g extract (absorbance at 510 nm).

2.6.5. Moisture content

Moisture content (%) was determined gravimetrically as $[(W_{wet} - W_{dry})/W_{wet}] \times 100$, where ~2 g samples were dried at 105 °C to constant mass.

2.6.6. Optical microscopy

Particle morphology was examined at ×400 magnification (Olympus CX23, Japan). The optimised and a representative non-optimised powder were compared for particle shape, surface texture, and aggregation.

2.7. Validation of optimised conditions

The RSM-predicted optimal conditions were validated experimentally in triplicate. A relative prediction error, calculated as the absolute difference between the predicted and experimentally observed values expressed as a percentage of the experimentally values, below 10% was adopted as the acceptance criterion (Bezerra et al., 2008).

2.8. Techno-economic analysis (TEA)

A structured TEA was conducted at two scales, with all input quantities derived directly from the experimental mass balance. At laboratory scale, one SD-2L Spray dryer (Zhengzhou Machine, China) run per day was modelled: feed volume = 9 mL/min × 150 min = 1,350 mL; *M. charantia* powder input = 135

g (1:10 w/v); maltodextrin input = 202.5 g (15% w/v); aqueous extract solubles ≈ 54 g; total dissolved solids (TDS) = 256.5 g; encapsulate output = 9.0% × 256.5 g = 23.1 g/day, where powder yield was calculated as the mass of dry encapsulate recovered from the collection vessel divided by the total dissolved solids mass fed into the dryer, expressed as a percentage. The pilot scale was defined as the output consistent with a 60-fold mass-balance scale-up, namely 1,400 g encapsulate/day requiring 8.19 kg *M. charantia* powder and 12.3 kg maltodextrin per day. This scale-up assumes linear mass-balance proportionality between laboratory and pilot output; in practice, energy efficiency and drying kinetics typically shift non-linearly with dryer size, so the pilot-scale figures represent a theoretical, first-order approximation rather than an outcome validated at industrial scale. Cost components comprised: (i) raw material costs at Malaysian market prices (*M. charantia* powder at MYR 110/kg retail, MYR 93.5/kg bulk with 15% volume discount; maltodextrin at MYR 15/kg retail, MYR 12/kg bulk); (ii) direct energy costs at MYR 0.435/kWh (Suruhanjaya Tenaga, 2023); laboratory: 1.5 kW SD-2L × 2.5 h plus ancillaries; pilot: 20 kW industrial dryer × 4 h plus ancillaries; (iii) labour at MYR 1,500/month ÷ 176 h (Jabatan Tenaga Kerja, 2023), giving an hourly wage rate of MYR 8.52/h ; laboratory: 4 active hours (MYR 34.08/day) ; pilot: 1.5 full time equivalent (FTE) worker × 8 h/day (MYR 102.27/day); (iv) straight-line depreciation (laboratory: MYR 15,000 over 5 years × 250 days/year = MYR 12.00/day; pilot scale dryer: MYR 180,000 = MYR 144.00/day); and (v) overhead at 20% of direct costs. Sensitivity analysis varied raw material cost (±20%), powder yield (±15%), and energy cost (±15%). Break-even volume was calculated as monthly fixed costs ÷ (selling price − variable cost per gram). The TEA represents a screening-level (TRL 3–4) analysis grounded in the experimental mass balance, not an investment-grade engineering estimate. The 9.0% laboratory-scale yield is below the 80–95% typical of industrial spray drying. This reflects the small bench-top SD-2L dryer used, where a high ratio of chamber surface area to feed throughput causes greater wall deposition and cyclone loss than industrial equipment. Larger-chamber dryers with more efficient cyclone separators would be expected to recover substantially more encapsulate per unit of feed. As the present TEA carries the 9.0% yield through to the pilot-scale projection, it likely understates the achievable cost efficiency at true industrial scale. Confirming this would require pilot validation on production-representative equipment, which falls outside the present TRL 3–4 screening-level scope.

2.9. Market diffusion modelling

A modified Gompertz diffusion model was applied to project cumulative market penetration of the encapsulated ingredient within the Malaysian functional food market (Meade & Islam, 2006). The Gompertz model is selected for its asymmetric growth profile, which features a prolonged initial adoption phase, subsequent acceleration, and a long convergence tail (Tattershall et al., 2021). This trajectory accurately reflects the market entry of a novel functional food ingredient. Unlike the symmetric acceleration and deceleration of the Logistic model, the Gompertz framework accounts for the extensive periods required for consumer education, regulatory familiarization, and manufacturer trust-building before uptake accelerates. A cumulative revenue is expressed as $N(t)=K\cdot\exp\{-\exp[-r(t-t0)]\}$, where K is the market ceiling (MYR million), r is the intrinsic adoption rate (yr^{-1}), and t_0 is the inflection time (yr). The base ceiling was set as K_{base} = MYR 4,100 million × 0.0005 = MYR 2.05 million (Euromonitor International, 2023). A 0.05% penetration rate was adopted to reflect the niche positioning of the encapsulated ingredient, which targets a specific diabetes-focused functional beverage segment rather than the broader functional food market as a whole. A broad-spectrum ingredient addressing multiple health claims across diverse product categories would instead warrant a substantially higher penetration rate from 0.1-0.5%. Niche, indication-specific functional ingredients typically achieve lower early-stage category penetration than multi-benefit ingredients, consistent with the conservative-to-optimistic bracket (0.035-0.065%; Table 8) used here to bound this uncertainty rather than assert a single value. The conservative ceiling (K = MYR 1.44 million; K_{base} × 0.70) and the optimistic ceiling (K = MYR 2.67 million; K_{base} × 1.30) reflect a ±30% market-penetration uncertainty. The growth rate r = 0.32 yr^{-1} was calibrated from ASEAN functional food ingredient adoption analogues (Meade & Islam, 2006); the conservative (r = 0.22 yr^{-1}) and optimistic (r = 0.42 yr^{-1}) values reflect a ±0.10 yr^{-1} bound. All N(t) values were computed analytically from the Gompertz equation, with t_0 representing the inflection time at which

$N(t_0) = K/e$ (≈36.8% of the ceiling), consistent with the asymmetric Gompertz profile rather than the symmetric 50% inflection of the Logistic model. We note as a limitation that the ASEAN analogue growth rates were adopted directly as the Gompertz r parameter without independent confirmation that the source analogues were themselves fitted using a Gompertz, rather than Logistic or Bass, diffusion function; because r is not necessarily interchangeable across functional forms with differing curvature, this represents a potential source of bias in the growth-rate calibration and is flagged for validation once post-launch sales data become available.

3. Results and Discussion

3.1. RSM model fitting and statistical validation

The sixteen experimental runs produced DPPH values ranging from 37.59% (Run 1: 30 min, gum arabic, 10%, 140 °C) to 58.31% (Run 6: 120 min, gum arabic, 15%, 140 °C), and powder yields from 6.54% to 10.50% (Table 2). The sixteen experimental runs produced DPPH values ranging from 37.59% (Run 1: 30 min, gum arabic, 10%, 140°C) to 58.31% (Run 6: 120 min, gum arabic, 15%, 140°C), and powder yields from 6.54% to 10.50% (Table 2**). These yields are markedly below the 80-95% typically reported for industrial spray drying; the underlying causes are addressed in Section 3.6.** The ANOVA results are summarised in Table 3. Overall model F-values of 4.88 (DPPH; $p = 0.047$) and 40.00 (yield; $p < 0.0001$) confirm statistical significance at $\alpha = 0.05$. R^2 values of 0.9071 (DPPH) and 0.9786 (yield) indicate that the fitted models explain more than 90% and 97% of the response variability, respectively; adjusted R^2 values of 0.7214 and 0.9541 corroborate these fits after penalising for model complexity. Adequate precision values of 7.872 (DPPH) and 13.927 (yield) both exceed the threshold of 4.0 (Yuan et al., 2023), and CV% values of 5.16% and 4.19% confirm satisfactory experimental reproducibility.

A critical limitation of the DPPH model requires explicit discussion. Its predicted R^2 of 0.0489 lies substantially below the adjusted R^2 of 0.7214 — a discrepancy that far exceeds the 0.20 threshold recommended by Myers et al. (2016) and is diagnostic of model overfitting within the design space, with severely limited extrapolation capacity. Probable causes include the narrow DPPH response range (a 20.7-percentage-point spread across 16 runs), the inherent assay variability associated with complex plant matrices, and the small design size ($n = 16$). This limitation is not merely a statistical footnote: the predicted DPPH optimum of 58.31% should be treated as a descriptive within-design indicator rather than an extrapolatable prediction, and the 8.11% experimental deviation reported in Section 3.4 must be interpreted accordingly. By contrast, the yield model showed excellent predicted-vs.-adjusted R^2 alignment (0.8882 vs. 0.9541), confirming robust predictive capability. The Predicted-vs.-Actual diagnostic plots (Fig. 7) visualise this asymmetry: the yield data (Fig. 7b) cluster tightly along the parity line across the full response range, whereas the DPPH data (Fig. 7a) exhibit visible scatter at intermediate values and one prominent low-end outlier corresponding to Run 1, consistent with the high extrapolation risk identified by the predicted-R^2 metric (Tyagi & Kumar, 2024; Zhao et al., 2023). Future studies should expand the design space, include at least three levels for extraction time, and incorporate a minimum of three centre-point replicates to mitigate the overfitting risk on the antioxidant response.

Despite this limitation, three lines of evidence support the reliability of the specific optimised condition identified here, as distinct from the model's general extrapolation capacity. First, triplicate experimental validation at the predicted optimum (Section 3.4) returned a DPPH relative error of 8.11%, within the conventionally accepted 10% threshold, indicating that the model retains adequate local accuracy at the specific point tested, even though its predicted R^2 signals unreliable performance when extrapolating to untested regions of the design space. Second, the optimum condition (117.67 min, 15% maltodextrin, 140°C) lies within the interior of the tested design space rather than at an extrapolated boundary, meaning the validated point is an interpolation, the regime in which RSM models are most reliable, rather than an extrapolation, the regime the low predicted R^2 specifically warns against. Third, the optimum is directionally consistent with the individually significant main effects (extraction time and inlet temperature, both $p < 0.05$) and the significant carrier loading × temperature interaction, rather than resulting from an isolated or counterintuitive combination of factors, reducing the likelihood that the optimum is an artefact of overfitting rather than a genuine local maximum. Accordingly, the reported

optimum and its experimental validation should be read as a reliable interpolated result specific to this design space, not as a generalisable predictive model; any application of the fitted equation beyond the tested ranges of extraction time, carrier loading, and inlet temperature would require independent re-validation.

3.2. Effect of process variables on DPPH antioxidant activity

Extraction time (A; $p = 0.0194$) and inlet temperature (D; $p = 0.0206$) exerted statistically significant individual effects on DPPH scavenging activity; the CD interaction (carrier loading × temperature; $p = 0.0266$) was also significant. By contrast, carrier type (B; $p = 0.1371$) and carrier loading (C; $p = 0.0576$) did not reach individual significance. Longer maceration (120 min vs. 30 min) consistently increased DPPH activity across all conditions, an outcome attributable to the progressive dissolution of polar phenolics and flavonoids from the cell matrix into the aqueous solvent (Monton & Luprasong, 2019; Oubannin et al., 2024) and consistent with the monotonic time–antioxidant dependence reported for related Malaysian plant systems under comparable maceration conditions (Mohd Sabry et al., 2024). It should be noted that 120 min represents the upper bound of the design space, and that DPPH activity showed no evidence of a plateau — it continued to increase monotonically with extraction time across the explored range. Future studies should therefore extend maceration to at least 180 min to characterise the full extraction kinetic profile and identify the true optimum or plateau.

The lower inlet temperature of 140 °C was consistently superior to 160 °C for DPPH retention, in agreement with the known thermal sensitivity of *M. charantia* phenolics. Mechanistically, at the higher inlet temperature the surface-to-core drying rate is no longer compatible with full bioactive retention: rapid surface evaporation accelerates crust formation on atomised droplets, which promotes core collapse, particle buckling, and degradation of trapped bioactives before complete drying is achieved (Maas et al., 2011; Mohammed et al., 2017; Tao et al., 2024). The significant CD interaction ($p = 0.0266$) reflects a protective synergy at the combined high-carrier-loading and low-temperature condition: at 140 °C with 15% maltodextrin, DPPH activities reached 58.31% and 57.63% (Runs 6 and 8), the two highest values in the design. The 3D response surface for DPPH (Fig. 4a) visualises the joint dependence on extraction time and inlet temperature, with the response maximised along the long-time / low-temperature edge of the design space.

One apparent anomaly deserves explicit note. Run 1 (30 min, gum arabic, 10%, 140 °C) yielded the lowest DPPH value (37.59%), whereas Run 9 (same extraction time, but 160 °C) yielded 54.12% — a reversal of the general temperature trend. It is very likely that this reversal reflects an inadequate matrix formation at 10% gum arabic combined with 140 °C: the carrier loading is insufficient to form a cohesive shell, and the lower thermal driving force is insufficient to complete the surface drying before the core collapses, producing powders with poor structural integrity and bioactive retention. At 160 °C, the faster surface drying at low carrier loading is at least able to fix particle morphology, partially compensating for the matrix inadequacy. This interpretation indirectly suggests that the interaction between carrier adequacy and the thermal regime at low loading warrants dedicated mechanistic investigation using differential scanning calorimetry (DSC) and direct quantification of encapsulation efficiency (EE%).

3.3. Effect of process variables on powder yield

Carrier loading dominated the powder yield with an F-value of 312.64 ($p < 0.0001$) — a magnitude that dwarfs all other effects and that directly reflects the proportionality between feed total-dissolved-solids and recovered powder mass. A 15% w/v loading produced yields of 9.80–10.50% versus 6.54–7.67% at 10% w/v, a consistent ~50% improvement across the design, and the corresponding 3D response surface (Fig. 4b) shows yield rising monotonically with carrier loading with only minor sensitivity to extraction time. At 10% loading, the encapsulating shell is likely insufficiently robust to withstand atomisation stresses, leading to wall collapse and the loss of fine particles to the dryer walls and the bag filter (Espinoza-Espinoza et al., 2024; Toprakçı et al., 2024). The overwhelming dominance of carrier loading on yield, combined with its non-significant individual effect on DPPH, identifies 15% maltodextrin as the unique condition at which both objectives are jointly maximised within the design space.

3.4. Optimised conditions and model validation

RSM numerical optimisation using the desirability function with equal weighting identified the following operating point: extraction time 117.67 min; carrier type maltodextrin; carrier loading 15% w/v; inlet temperature 140 °C (composite desirability = 0.968). The predicted responses were DPPH = 58.31% and yield = 10.13% (Table 4). Triplicate experimental validation returned DPPH = 53.58 ± 1.24% and yield = 9.00 ± 0.45%, corresponding to relative errors of 2FI% and 11.15%. The DPPH error sits within the conventionally accepted 10% threshold. The yield error of 11.15% is marginally above threshold but is mechanistically explicable by the laboratory-scale cyclone collection variability at the boundary condition of 15% carrier loading and is consistent with the 5–12% validation error range reported in comparable spray-drying optimisation studies (Goyal et al., 2020; Toprakçı et al., 2024). The visual appearance of the validated encapsulate produced under the optimum conditions is shown in Fig. 5a as a free-flowing off-white powder; Fig. 5b contrasts this with a representative non-optimised batch (160 °C, 10% gum arabic, 30 min) that appears darker and more agglomerated, providing a macroscopic preview of the morphological differences quantified by microscopy in Section 3.5.3. The agreement between predicted and experimental responses is considered acceptable for the present purpose of identifying a commercially scalable operating point.

3.5. Physicochemical and phytochemical characterisation

3.5.1. Total phenolic and flavonoid content

The optimised encapsulate exhibited TPC of 3.07×10^{-4} g GAE/g extract and TFC of 6.99×10^{-4} g QE/g extract (Table 5). These values are consistent with reports for aqueous *M. charantia* extracts encapsulated with maltodextrin at similar solid-to-solvent ratios (Goyal et al., 2020), and their preservation within the maltodextrin matrix is in good agreement with the documented protective role of high-molecular-weight polysaccharide carriers against oxidative degradation during drying (Arenas-Jal et al., 2020). The values are substantially lower than those reported for organic-solvent (ethanol/methanol) extracts, which typically yield 5–20-fold higher phenolic concentrations (Jia et al., 2017). This discrepancy is expected and is a direct consequence of solvent selection: aqueous extraction selectively recovers highly polar, water-soluble phenolics while excluding lipophilic constituents — a deliberate choice here to maintain food-grade safety and beverage matrix compatibility. It should also be noted that several of the constituents emphasised in Fig. 1 (charantin, momordicin, cucurbitacins) are lipophilic and are not efficiently recovered by the aqueous protocol used here; the present encapsulate therefore concentrates the polar antioxidant fraction of the *M. charantia* phytochemical inventory, while the lipophilic hypoglycaemic constituents are addressed in a parallel ethanolic-extract study to be reported elsewhere. Future work should investigate aqueous-ethanol co-solvents (50–70% v/v) and employ LC-MS/MS for comprehensive phenolic profiling to enable quantitative cross-study comparison.

3.5.2. Moisture content

The moisture content of 2.04% is well within the ≤ 3% specification commonly adopted for spray-dried plant extract powders (Ferrari et al., 2012). Low moisture content minimises the water activity (a_w), reducing the risk of microbial proliferation, enzymatic activity, and Maillard browning (Michalska & Lech, 2018), and it maintains the glass transition temperature (T_g) above storage temperature to prevent caking, stickiness, and accelerated bioactive degradation (Germano et al., 2009; Goula & Adamopoulos, 2010). The outlet temperature of approximately 85 °C achieved under the optimum conditions is consistent with published values for maltodextrin-based polyphenol encapsulation (Mohammed et al., 2017). Multi-layer aluminium moisture-barrier sachets with desiccant are recommended for long-term storage of the powder.

3.5.3. Particle morphology

Optical microscopy revealed marked morphological differences between the non-optimised and the optimised powders (Fig. 6), and the contrast offers a clear illustration of the structure–property–functionality relationship that underpins encapsulate performance. The non-optimised powder (Fig. 6a; 160 °C, 10% gum arabic, 30 min) exhibited irregular, agglomerated particles with rough, folded, or concave surfaces — the characteristic signature of a high droplet Péclet number, in which rapid surface evaporation creates a rigid crust before the core has fully dried, leading to buckling under the subsequent

vapour-pressure-driven contraction (Baldinger et al., 2012; Maas et al., 2011). The optimised powder (Fig. 6b; 140 °C, 15% maltodextrin, 117.67 min) exhibited near-spherical particles with smoother, more uniform surfaces, attributable to the lower drying intensity and the more cohesive maltodextrin shell. Mechanistically, the lower inlet temperature reduces the surface-to-core drying gradient, while the higher carrier loading provides sufficient polysaccharide mass to form a continuous shell that resists buckling — the structural feature that dictates the property (apparent density, surface uniformity) and, in turn, the functionality (rapid dissolution in aqueous beverage matrices and improved flowability during downstream handling) (Toprakçı et al., 2024). **Optical microscopy at ×400 magnification was sufficient to resolve gross particle shape and agglomeration, the level of detail needed to distinguish the optimised from the non-optimised powder here. However, this technique cannot resolve sub-micron surface texture, wall porosity, or fine surface fissures that influence encapsulation integrity and moisture ingress.** Therefore, future studies should employ scanning electron microscopy (SEM) and laser diffraction particle-size analysis (D_{10}, D_{50}, D_{90}) for quantitative morphological characterisation.

3.6. Techno-economic analysis

A mass-balance-grounded TEA was conducted at the laboratory and projected pilot scale, with all input quantities derived directly from the experimental protocol and yield data (Table 6). At laboratory scale, one full SD-2L Spray dryer run per day (1,350 mL feed; 135 g *M. charantia* powder; 202.5 g maltodextrin; TDS = 256.5 g) yields 23.1 g encapsulate/day at 9.0% yield. **The low yield reflects the small chamber size of the bench-top SD-2L dryer (2 L) relative to industrial units. In a small chamber, atomised particles travel only a short distance before contacting the chamber wall, where a substantial fraction adheres rather than reaching the cyclone separator for collection. Industrial-scale dryers have proportionally larger chambers, allowing particles more distance and time to dry fully before collection, and therefore typically achieve the 80-95% yields reported in the literature.**

Fruit and plant extract also are often rich in sugars, organic acids, and other low-molecular-weight compounds with low glass transition temperature (Tg). When the dried particle surface temperature exceeds its Tg during drying, the particle becomes sticky and adheres to the chamber wall instead of remaining free-flowing, which directly reduces yield (Ocampo et al., 2025). The pilot scale represents a 60-fold mass-balance scale-up, yielding 1,400 g encapsulate/day from 8.19 kg *M. charantia* powder and 12.3 kg maltodextrin.

At laboratory scale, the unit cost of MYR 3.66/g is dominated by labour (40.3% of total cost), reflecting the low output-to-effort ratio of single small-batch processing. At pilot scale, the unit cost falls to MYR 1.14/g — a 3.2-fold reduction — driven by improved labour productivity and the distribution of depreciation across a 60-fold larger output. Raw material cost becomes the dominant component at pilot scale (56.5% of total), identifying raw-material procurement strategy and yield improvement as the highest-priority cost-reduction targets.

The sensitivity analysis (Table 7) confirmed that the unit cost is most sensitive to yield variation (±15% yields a −13.0% to +17.6% unit-cost change) and to raw material cost (±20% yields ±11.5%). Energy cost has negligible impact (±1.1%), confirming robust insensitivity to electricity-price fluctuation. These sensitivities directly inform future R&D priorities: improving yield from 9.0% toward 12–15% through optimised atomisation conditions or enhanced carrier formulations would deliver more unit-cost reduction than any other single improvement.

Break-even analysis at pilot scale identified monthly fixed costs of MYR 3,168 (depreciation × 22 working days); depreciation is treated as the sole formal fixed-cost line item at this screening level, with rent, insurance, and salaried management not itemised separately and implicitly absorbed within the 20% overhead allocation (Table 6) — itemised fixed-cost accounting is identified as a requirement for the full pilot-scale TEA in Section 3.9. The variable cost per gram used in the break-even calculation (MYR 1.04/g) comprises raw materials, energy, labour, and overhead — i.e., the pilot-scale unit cost of MYR 1.14/g (Table 6) less its depreciation component (MYR 0.10/g) — so that fixed and variable costs are not double-counted. At a retail price of MYR 8.00/g, break-even occurs at approximately 0.4 kg/month; at MYR 5.00/g, approximately 0.8 kg/month. Both volumes represent less than 3% of the pilot-scale monthly production capacity (30.8 kg/month = 1,400 g/day × 22 days), confirming that commercial

viability is achievable even at minimal demand levels. Comparable Malaysian encapsulated plant-extract ingredients are priced at MYR 6–12/g retail (Euromonitor International, 2023), supporting the market-competitive positioning of the MYR 8.00/g benchmark used here. Positioning these results against comparable spray-dried botanical encapsulation systems clarifies both the yield gap and the cost implication it carries. Tan et al. (2015) achieved a substantially higher process yield (66.2% ± 9.4%) encapsulating aqueous *M. charantia* extract with maltodextrin/Arabic gum, though at a considerably higher carrier solids loading (35% w/w) than used here (10-15% w/v); similarly, Ferro et al. (2020) reported 59-65% yield for *Sida rhombifolia* extract encapsulated with maltodextrin at 20-25% w/w. The present study's 9.0% optimum yield sits well below both benchmarks, consistent with the lower carrier loading and smaller-scale bench-top equipment discussed in Section 3.3. Quantitative cost benchmarks for spray-dried botanical encapsulation, however, remain largely absent from the literature; neither Tan et al. (2015) nor Ferro et al. (2020), nor other comparable studies identified, report a per-gram production cost or techno-economic analysis alongside their yield data, underscoring the gap this study's TEA is intended to address (Section 1).

3.7. Market diffusion modelling

Gompertz diffusion projections under three scenarios are presented in Table 8. All N(t) values were computed analytically from $N(5) = K \cdot \exp\{-\exp[-r(5 - t_0)]\}$ using K_{base} = MYR 4,100 million × 0.0005 = MYR 2.05 million. The conservative ceiling (K = MYR 1.44 million; K_{base} × 0.70) and the optimistic ceiling (K = MYR 2.67 million; K_{base} × 1.30) reflect ±30% bounds on market penetration.

Under the base scenario, cumulative market revenue reaches MYR 1.04 million at year 5, with the maximum adoption rate at $t_0 \approx 3.8$ years post-commercial launch — a timeline consistent with the typical regulatory approval, consumer-awareness, and distribution-establishment trajectory for novel functional food ingredients in Malaysia. These projections should be interpreted as scenario-based estimates rather than definitive indicators of commercial feasibility, since the market ceiling (K), penetration rate, and growth-rate parameter (r) were all calibrated from category-level market data and analogous ingredient launches rather than direct sales data for this specific product. The conservative, base, and optimistic scenarios (Table 8) are presented to bound this uncertainty, not to represent a single predicted outcome. Under the base case, the pilot-scale capital investment of MYR 180,000 represents a modest 17.3% of the projected 5-year cumulative revenue, suggesting a potentially favourable return profile subject to operational efficiency and actual production ramp-up; a definitive payback period requires a discounted, year-by-year net-cash-flow analysis rather than a simple investment-to-revenue ratio, and is identified as a priority for the full pilot-scale TEA (Section 3.9). The National Pharmaceutical Industry Blueprint 2021–2030 (Malaysian Investment Development Authority, 2021) and the JAKIM Halal certification frameworks provide additional enabling conditions for market entry. Validation of the growth-rate parameter with post-launch sales data will be essential once commercial production begins.

3.8. Implications for functional food applications

The optimised *M. charantia* spray-dried encapsulate exhibits the four properties needed for functional beverage and food-system applications: a moisture content of 2.04% supports storage stability; the near-spherical morphology supports rapid dissolution and good flowability; the confirmed phenolic and flavonoid content provides a measurable bioactive payload; and the food-grade maltodextrin carrier supports regulatory compliance. Recent Malaysian consumer-preference work on functional food powders — including a study of Olivetin-based powdered formulations (Bashir et al., 2024) — confirms that consumer acceptability of novel encapsulated ingredients in a powdered, beverage-compatible format is achievable, although a formal sensory panel evaluation of the present encapsulate remains a required follow-up. The naturally bitter taste of crude *M. charantia* extract is expected to be attenuated by the maltodextrin encapsulation matrix and by the flavour-masking capacity of typical beverage matrices (Khandaker et al., 2020; Shahbazi et al., 2018), although a formal sensory panel evaluation is required to confirm this. Taken together with the unit cost of MYR 1.14/g at projected pilot scale, the optimised encapsulate is technically and economically positioned for integration into beverage formulations for the Malaysian and ASEAN functional food markets. This potential is based on the process characteristics, projected cost, and market analysis presented in this study, together with the well-documented

phytochemical profile of *M. charantia*. However, the present study does not establish antidiabetic efficacy of the encapsulate itself, as direct α-glucosidase and α-amylase inhibition, bioaccessibility, and other relevant bioactivity assays were not performed. These evaluations are therefore identified as priorities for future work.

3.9. Limitations and future research priorities

Five limitations of the present work define an explicit forward research agenda. First, direct quantification of encapsulation efficiency (EE%) using solvent washing or DSC is needed and represents an important area for future investigation to establish how much core material is genuinely wall-protected versus surface-exposed. The present work establishes powder recovery yield and post-encapsulation total phenolic and flavonoid contents (TPC/TFC), providing bulk-level process and compositional characterisation of the optimised encapsulate. This additional measurement would strengthen the characterisation of the encapsulation process and provide a basis for subsequent evaluation of storage stability, bioactive release, and oxidative protection. Second, in vitro bioaccessibility studies using the validated INFOGEST protocol are needed to confirm physiologically relevant bioactive release during gastrointestinal transit, together with α-glucosidase and α-amylase inhibition assays to directly substantiate the hypoglycaemic claim. Third, a full pilot-scale TEA incorporating actual supplier quotations, pilot-dryer yield data, and regulatory compliance costs is needed before investment decisions can be made — the present analysis is a screening-level (TRL 3–4) first estimate, not a final investment case. Fourth, sensory evaluation of beverages formulated with the encapsulate is needed, with attention to residual bitterness and consumer perception. Fifth, accelerated storage stability testing (40 °C / 75% RH over 3 months) is required to substantiate the shelf-stable claim. Sixth, the present study used a two-level full factorial design without centre or axial points and therefore could not estimate quadratic (curvature) effects; a true Central Composite Design with at least three centre-point replicates is recommended in future work to enable second-order model fitting, lack-of-fit testing, and more robust extrapolation beyond the tested design space. Together these six priorities map a coherent translational pathway from the optimised laboratory protocol toward clinically and commercially validated functional food products.

4. Conclusions

In this work, the coupled aqueous maceration and spray-drying microencapsulation of *Momordica charantia* fruit extract was optimised by RSM using a two-level full factorial design (RSM–FFD) and, critically, this optimisation was coupled with a mass-balance-grounded techno-economic analysis and a modified Gompertz market diffusion model — bridging process characterisation with commercial viability in a single analytical framework. Under the optimum conditions (extraction time 117.67 min; maltodextrin 15% w/v; inlet temperature 140 °C), the encapsulate exhibited DPPH scavenging activity of 53.58 ± 1.24%, powder yield of 9.00 ± 0.45%, TPC of 3.07×10^{-4} g GAE/g extract, TFC of 6.99×10^{-4} g QE/g extract, and moisture content of 2.04%, with near-spherical morphology consistent with a low droplet Péclet number and a cohesive maltodextrin shell. Mechanistically, the lower inlet temperature combined with the higher carrier loading reduces the surface-to-core drying gradient and provides sufficient polysaccharide mass to form a continuous shell that resists buckling — the structural feature that dictates the dissolution and flowability properties needed for functional beverage formulation. The mass-balance-grounded TEA returned a laboratory-scale unit cost of MYR 3.66/g (USD 0.78/g; 23.1 g/day) and a pilot-scale unit cost of MYR 1.14/g (USD 0.24/g; 1,400 g/day) — a 3.2-fold scale reduction — with break-even achieved below 0.8 kg/month under conservative pricing. The Gompertz model projects cumulative revenue of MYR 0.59–1.67 million at year 5 (base case MYR 1.04 million); the pilot-scale capital investment represents a modest 17.3% of this projected 5-year revenue, suggesting a potentially favourable return profile pending a full discounted cash-flow analysis. The low predicted R^2 of the DPPH model (0.0489) is acknowledged as the principal statistical limitation, requiring an expanded design space in future studies. The coupled framework demonstrated here — RSM optimisation, mass-balance-grounded TEA, and Gompertz diffusion modelling — provides a generalisable template for designing future plant-bioactive encapsulation processes guided by quantitative cost and market trajectories from the outset.

Conflict of Interest

No conflict of interest has been declared by the authors.

Acknowledgements

This study was supported by an industry–university collaborative research grant between EMZI Holding Sdn Bhd and Universiti Teknologi MARA (UiTM) grant no MIH (008/2020). The authors gratefully acknowledge the facilities and technical support provided by the EMZI–UiTM Nanoparticles, Colloids and Interface Industrial Research Laboratory (NANO-CORE), UiTM Cawangan Pulau Pinang, Kampus Permatang Pauh. The funders had no role in the design, collection, analysis, or interpretation of data; in the writing of the manuscript; or in the decision to publish.

References

American Diabetes Association. (2023). Standards of care in diabetes — 2023. Diabetes Care, 46(Suppl. 1), S1–S291. https://doi.org/10.2337/dc23-Sint

Arenas-Jal, M., Suñé-Negre, J. M., & García-Montoya, E. (2020). An overview of microencapsulation in the food industry. European Food Research and Technology, 246(7), 1371–1382. https://doi.org/10.1007/s00217-020-03496-x

Baldinger, A., Clerdent, L., Rantanen, J., Yang, M., & Grohganz, H. (2012). Quality by design approach in the optimization of the spray-drying process. Pharmaceutical Development and Technology, 17(4), 389–397. https://doi.org/10.3109/10837450.2010.550623

Başar Altinterim, B. (2012). Bitter melon (Momordica charantia) and the effects on diabetes. Journal of Agricultural Faculty of Uludag University, 26(2), 65–70.

Bashir, M. A. A., Osman, M. S., Wahab, M. S. A., Burhan, N. S., Ismail, A. K., & Mohd Rusli, M. N. F. (2024). Quantifying consumers' acceptance of functional foods in powdered form: A study of Olivetin. International Journal of Academic Research in Business and Social Sciences, 14(7), 1–12.

Bezerra, M. A., Santelli, R. E., Oliveira, E. P., Villar, L. S., & Escaleira, L. A. (2008). Response surface methodology (RSM) as a tool for optimization in analytical chemistry. Talanta, 76(5), 965–977. https://doi.org/10.1016/j.talanta.2008.05.019

Brand-Williams, W., Cuvelier, M. E., & Berset, C. (1995). Use of a free radical method to evaluate antioxidant activity. LWT — Food Science and Technology, 28(1), 25–30. https://doi.org/10.1016/S0023-6438(95)80008-5

Caro-Ordieres, T., Marín-Royo, G., Opazo-Ríos, L., Jiménez-Castilla, L., Moreno, J. A., Gómez-Guerrero, C., & Egido, J. (2020). The coming age of flavonoids in the treatment of diabetic complications. Journal of Clinical Medicine, 9(2), 346. https://doi.org/10.3390/jcm9020346

Chang, C. C., Yang, M. H., Wen, H. M., & Chern, J. C. (2002). Estimation of total flavonoid content in propolis by two complementary colorimetric methods. Journal of Food and Drug Analysis, 10(3), 178–182.

Cilek, B., Luca, A., Hasirci, V., Sahin, S., & Sumnu, G. (2012). Microencapsulation of phenolic compounds extracted from sour cherry pomace. European Food Research and Technology, 235(4), 587–596. https://doi.org/10.1007/s00217-012-1786-8

Espinoza-Espinoza, L. A., Muñoz-More, H. D., et al. (2024). Microencapsulation of vitamins: A review and meta-analysis of coating materials, release, and food fortification. Food Research International, 178, 114420. https://doi.org/10.1016/j.foodres.2024.114420

Euromonitor International. (2023). Health and Wellness in Malaysia: Market Report 2023. Euromonitor International, London.

Fadil, N. A., Zul-kharnain, S. N., Wahab, M. S. A., Sembada, A. A., Osman, M. S., et al. (2025). Advancing green chemistry through ultrasound-assisted extraction of flavonoids from Moringa oleifera using response surface methodology. Sustainable Chemistry One World, 5, 100115. https://doi.org/10.1016/j.scowo.2025.100115

Ferrari, C. C., Germer, S. P. M., & de Aguirre, J. M. (2012). Effects of spray-drying conditions on the physicochemical properties of blackberry powder. Drying Technology, 30(2), 154–163. https://doi.org/10.1080/07373937.2011.628429

Ferro, D. M., Müller, C. M. O., & Ferreira, S. R. S. (2020). Photostability and characterization of spray-dried maltodextrin powders loaded with *Sida rhombifolia* extract. *Biocatalysis and Agricultural Biotechnology*, *27*, Article 101716. https://doi.org/10.1016/j.bcab.2020.101716

Germano, M. A., Souza, A. S., Edy, M., & Azeredo, H. M. C. (2009). Physical properties of spray-dried acerola pomace extract. LWT — Food Science and Technology, 42(2), 641–645. https://doi.org/10.1016/j.lwt.2008.07.008

Goula, A. M., & Adamopoulos, K. G. (2010). A new technique for spray-drying orange juice concentrate. Innovative Food Science & Emerging Technologies, 11(2), 342–351. https://doi.org/10.1016/j.ifset.2009.12.001

Goyal, S., Sonawane, S. K., Nachal, N., & Arya, S. S. (2020). Encapsulation of Momordica charantia Linn. (bitter gourd) juice by spray-drying technique. Journal of Food Measurement and Characterization, 14(6), 3529–3541. https://doi.org/10.1007/s11694-020-00599-7

Institute for Public Health. (2019). National Health and Morbidity Survey 2019: Non-Communicable Diseases, Healthcare Demand, and Health Literacy. Ministry of Health Malaysia.

International Diabetes Federation. (2021). IDF Diabetes Atlas (10th ed.). International Diabetes Federation. https://www.diabetesatlas.org

Ismail, M. H. A., Osman, M. S., Khairudin, K., Zainon, M. F., Mohd Eusoff, A. F., & Zubli, Q. (2022). Statistical optimisation for the formulation of edible bird nest-based instant soup using Response Surface Methodology (RSM). Malaysian Journal of Chemical Engineering and Technology (MJCET), 5(2), 115–122.

Jabatan Tenaga Kerja. (2023). Minimum Wages Order 2022. Ministry of Human Resources, Malaysia.

Jia, S., Shen, M., Zhang, F., & Xie, J. (2017). Recent advances in Momordica charantia: Functional components and biological activities. International Journal of Molecular Sciences, 18(12), 2555. https://doi.org/10.3390/ijms18122555

Khandaker, M. U., Zainuddin, N. K., Bradley, D. A., et al. (2020). Radiation dose to the Malaysian populace via the consumption of roasted, ground, and instant coffee. Radiation Physics and Chemistry, 173, 108886. https://doi.org/10.1016/j.radphyschem.2020.108886

Kozłowska, M., & Gruczyńska, E. (2018). Effect of drying temperature on phenolic compound stability and antioxidant activity in plant materials. Chemical Papers, 72(10), 2607–2615. https://doi.org/10.1007/s11696-018-0516-5

Maas, S. G., Schaldach, G., Littringer, E. M., et al. (2011). The impact of spray-drying outlet temperature on the particle morphology of mannitol. Powder Technology, 213(1–3), 27–35. https://doi.org/10.1016/j.powtec.2011.06.024

Malaysian Investment Development Authority. (2021). National Pharmaceutical Industry Blueprint 2021–2030. Ministry of Investment, Trade and Industry, Malaysia.

Malik, R. A., Saad, M. M., & Tiwari, S. (2019). Effect of Extraction Time and Solvent Power on Phytochemical Screening and Antioxidant Activity of Momordica charantia L. Fruit Extracts. *Asian Journal of Chemistry*, *31*(3), 647–650. https://doi.org/10.14233/ajchem.2019.21715

Meade, N., & Islam, T. (2006). Modelling and forecasting the diffusion of innovation — a 25-year review. International Journal of Forecasting, 22(3), 519–545. https://doi.org/10.1016/j.ijforecast.2006.01.005

Michalska, A., & Lech, K. (2018). The effect of carrier quantity and drying method on the physical properties of apple juice powders. Beverages, 4(1), 2. https://doi.org/10.3390/beverages4010002

Ministry of Health Malaysia. (2020). Malaysia Health at a Glance 2020. Institute for Public Health, National Institutes of Health Malaysia.

Mirmiran, P. (2014). Functional foods-based diet as a novel dietary approach for management of type 2 diabetes. World Journal of Diabetes, 5(3), 267–281. https://doi.org/10.4239/wjd.v5.i3.267

Mohammed, N. K., Tan, C. P., Manap, Y. A., Alhelli, A. M., & Hussin, A. S. M. (2017). Process conditions of spray-drying microencapsulation of Nigella sativa oil. Powder Technology, 315, 1–14. https://doi.org/10.1016/j.powtec.2017.03.045

Mohd Sabry, M. I., Wahab, M. S. A., Osman, M. S., & Ismail, A. K. (2024). Statistical optimization of antioxidant and extraction yield from Centella asiatica leaves. International Journal of Innovation and Industrial Revolution, 6(17), 206–219.

Monton, C., & Luprasong, C. (2019). Effect of temperature and duration of maceration on nitrate content of Vernonia cinerea (L.) Less. International Journal of Food Science, 2019, 1281635. https://doi.org/10.1155/2019/1281635

Myers, R. H., Montgomery, D. C., & Anderson-Cook, C. M. (2016). Response Surface Methodology: Process and Product Optimization Using Designed Experiments (4th ed.). John Wiley & Sons.

Ocampo, V. P., Hernandez, A. L. Y., Marratte, R., Baena, Y., Gutiérrez-López, G. F., Ambrose, K., & Carvajal, M. T. (2025). Effect of drying methods on the physical and surface properties of blueberry and strawberry fruit powders: a review. *Applied Sciences*, *15*(24), 13094. https://doi.org/10.3390/app152413094

Oubannin, S., Bijla, L., et al. (2024). Recent advances in the extraction of bioactive compounds from plant matrices. Journal of Food Composition and Analysis, 128, 105995. https://doi.org/10.1016/j.jfca.2024.105995

Shahbazi, H., Hashemi Gahruie, H., Golmakani, M.-T., Eskandari, M. H., & Movahedi, M. (2018). Effect of medicinal plant type and concentration on properties of kombucha. Food Science & Nutrition, 6(8), 2568–2577. https://doi.org/10.1002/fsn3.873

Singleton, V. L., & Rossi, J. A. (1965). Colorimetry of total phenolics with phosphomolybdic–phosphotungstic acid reagents. American Journal of Enology and Viticulture, 16(3), 144–158.

Suruhanjaya Tenaga (Energy Commission Malaysia). (2023). Electricity Tariff Schedule. ST Malaysia.

Tan, S. P., Kha, T. C., Parks, S. E., Stathopoulos, C. E., & Roach, P. D. (2015). Effects of the spray-drying temperatures on the physiochemical properties of an encapsulated bitter melon aqueous extract powder. *Powder Technology*, *281*, 65–75. https://doi.org/10.1016/j.powtec.2015.04.074

Tan, S. P., Kha, T. C., Parks, S., Stathopoulos, C., & Roach, P. D. (2015). Optimising the encapsulation of an aqueous bitter melon extract by spray-drying. *Foods*, *4*(3), 400-419. https://doi.org/10.3390/foods4030400

Tao, Y., Tang, Z., Huang, Q., et al. (2024). Effects of spray-drying temperature on the physicochemical properties of grapeseed oil microcapsules. LWT — Food Science and Technology, 193, 115779. https://doi.org/10.1016/j.lwt.2024.115779

Tattershall, E., Nenadic, G., & Stevens, R. D. (2021). Modelling trend life cycles in scientific research using the Logistic and Gompertz equations. *Scientometrics*, *126*(11), 9113–9132. https://doi.org/10.1007/s11192-021-04137-0

Toprakçı, İ., Güngör, K. K., Torun, M., & Şahin, S. (2024). Spray-drying microencapsulation of plum-peel bioactives using gum arabic and maltodextrin. Food Bioscience, 61, 104824. https://doi.org/10.1016/j.fbio.2024.104824

Tyagi, P. K., & Kumar, V. (2024). Optimisation of spray-drying process parameters for encapsulation of plant bioactives: A comprehensive review. Food Research International, 175, 113762.

Yousafzai, A. K., Khan, M. I., Wahab, M. M. A., Adedeji, J. A., Feikie, X. E., & Yaro, N. S. A. (2026). RSM-Based modelling and optimization of the synergistic effects of waste tyre metal fibre on the electrical resistivity and mechanical properties of asphalt mixes. *Polymers*, *18*(9), 1042. https://doi.org/10.3390/polym18091042

Yuan, X., He, C., Xue, X., Liang, Z., & Chen, Y. (2023). Optimisation study on the flavonoid extraction process from Abrus precatorius leaves. Journal of Holistic Integrative Pharmacy, 4(2), 119–126. https://doi.org/10.1016/j.jhip.2023.09.003

Zahoor, I., Mir, T. A., Ganaie, T. A., Allai, F. M., Ayoub, W. S., & Farooq, S. (2024). Antidiabetic potential from selected Himalayan underutilised herbs: A review. Food and Humanity, 2, 100297. https://doi.org/10.1016/j.foohum.2024.100297

Zhao, X., et al. (2023). Application of response surface methodology for optimisation of spray-drying microencapsulation of plant polyphenols. LWT — Food Science and Technology, 185, 114998.

Tables

Table 1. Independent variables and their coded and actual levels in the two-level full factorial design.

Factor	Variable	Units	Type	Low (−1)	High (+1)
A	Extraction time	min	Numeric	30	120
B	Carrier type	—	Categorical	Gum arabic	Maltodextrin
C	Carrier loading	% (w/v)	Numeric	10	15
D	Inlet air temperature	°C	Numeric	140	160

Table 2. Two-level full factorial design experimental runs with observed DPPH scavenging activity and powder yield responses.

Std	Run	Ext. time (min)	Carrier	Loading (%)	Inlet T (°C)	DPPH (%)	Yield (%)
1	5	30	Gum arabic	10	140	37.59	6.93
2	13	120	Gum arabic	10	140	49.56	6.54
3	2	30	Maltodextrin	10	140	50.00	6.74
4	12	120	Maltodextrin	10	140	49.30	7.50
5	9	30	Gum arabic	15	140	48.97	10.11
6	3	120	Gum arabic	15	140	58.31	10.46
7	7	30	Maltodextrin	15	140	51.79	10.22

8	11	120	Maltodextrin	15	140	57.63	9.99
9	16	30	Gum arabic	10	160	54.12	6.65
10	10	120	Gum arabic	10	160	55.81	7.52
11	6	30	Maltodextrin	10	160	56.22	6.76
12	15	120	Maltodextrin	10	160	55.35	7.67
13	1	30	Gum arabic	15	160	51.63	10.50
14	4	120	Gum arabic	15	160	55.69	9.80
15	8	30	Maltodextrin	15	160	52.52	10.50
16	14	120	Maltodextrin	15	160	58.11	10.30

Table 3. ANOVA summary for the fitted RSM models for DPPH scavenging activity and powder yield.

Source	DPPH: F-value	DPPH: p-value	Yield: F-value	Yield: p-value
Model	4.88	0.0470*	40.00	<0.0001*
A — Extraction time	11.52	0.0194*	0.90	0.3750
B — Carrier type	3.13	0.1371	0.65	0.4451
C — Carrier loading	6.03	0.0576	312.64	<0.0001*
D — Inlet temperature	11.14	0.0206*	0.70	0.4304
AB	2.50	0.1746	0.59	0.4678
AC	1.37	0.2942	4.11	0.0824
AD	2.16	0.2017	0.073	0.7952
BC	0.59	0.4778	0.38	0.5577
CD	9.66	0.0266*	—	—
R^2	0.9071	—	0.9786	—
Adj. R^2	0.7214	—	0.9541	—
Pred. R^2	0.0489	—	0.8882	—
CV (%)	5.16	—	4.19	—
Adeq. precision	7.872	—	13.927	—

*Statistically significant at $p < 0.05$.

Table 4. RSM-predicted and experimentally validated conditions at the identified optimum (mean ± SD, n = 3).

Parameter	Predicted value	Experimental value	Relative error (%)
Extraction time (min)	117.67	117.67 (fixed)	—
Carrier type	Maltodextrin	Maltodextrin	—
Carrier loading (% w/v)	15.00	15.00 (fixed)	—
Inlet air temperature (°C)	140.0	140.0 (fixed)	—
DPPH scavenging activity (%)	58.31	53.58 ± 1.24	8.11
Powder yield (%)	10.13	9.00 ± 0.45	11.15

Relative error = |Predicted − Experimental| / Predicted × 100.

Table 5. Phytochemical and physicochemical characterisation of the optimised spray-dried encapsulate (mean ± SD, n = 3).

Parameter	Value	Unit
DPPH radical scavenging activity	53.58 ± 1.24	%
Antioxidant capacity (AA equivalent)	2.68 ± 0.08	g AAE/g extract
Total phenolic content (TPC)	$3.07 \times 10^{-4} \pm 0.12 \times 10^{-4}$	g GAE/g extract
Total flavonoid content (TFC)	$6.99 \times 10^{-4} \pm 0.18 \times 10^{-4}$	g QE/g extract
Moisture content	2.04 ± 0.11	%
Powder yield	9.00 ± 0.45	%
Optimal process conditions	117.67 min / Maltodextrin 15% w/v	—

			/ 140 °C

AAE = ascorbic acid equivalent; GAE = gallic acid equivalent; QE = quercetin equivalent.

Table 6. Techno-economic analysis at laboratory (23.1 g/day) and pilot scale (1,400 g/day). All inputs derived from the experimental mass balance.

Cost component	Lab scale	Pilot scale	Basis and notes
M. charantia powder	MYR 14.85	MYR 765.50	MYR 110/kg retail; MYR 93.5/kg bulk (−15%); 135 g / 8,190 g
Maltodextrin (DE 10–12)	MYR 3.04	MYR 147.37	MYR 15/kg retail; MYR 12/kg bulk; 202.5 g / 12,281 g
Water & consumables	MYR 2.00	MYR 80.00	Estimate
Direct energy	MYR 4.50	MYR 95.00	MYR 0.435/kWh; Lab: 1.5 kW × 2.5 h; Pilot: 20 kW × 4 h + ancillaries
Labour	MYR 34.09	MYR 102.27	MYR 1,500/month ÷ 176 h; Lab: 4 h active; Pilot: 1.5 FTE × 8 h
Depreciation	MYR 12.00	MYR 144.00	Lab: MYR 15,000 ÷ (5 yr × 250 days); Pilot: MYR 180,000 dryer
Overhead (20%)	MYR 14.10	MYR 266.83	20% of all direct costs
Total batch cost	MYR 84.57	MYR 1,601.00	
Encapsulate output	23.1 g/day	1,400 g/day	9.0% yield × TDS
Unit cost	MYR 3.66/g	MYR 1.14/g	3.2× scale reduction
Unit cost (USD)	USD 0.78/g	USD 0.24/g	USD/MYR = 4.68 (BNM, 2024)

Table 7. Sensitivity analysis: impact of key variable changes on pilot-scale unit cost (MYR/g).

Variable	Change	Unit cost (MYR/g)	Δ Unit cost (%)
Raw material cost	−20%	MYR 1.01/g	−11.5%
Raw material cost	Base	MYR 1.14/g	—
Raw material cost	+20%	MYR 1.27/g	+11.5%
Powder yield	−15%	MYR 1.35/g	+17.6%
Powder yield	Base	MYR 1.14/g	—
Powder yield	+15%	MYR 0.99/g	−13.0%
Energy cost	−15%	MYR 1.13/g	−1.1%
Energy cost	Base	MYR 1.14/g	—
Energy cost	+15%	MYR 1.16/g	+1.1%

Table 8. Modified Gompertz diffusion model parameters and scenario projections. N(t) denotes cumulative revenue from launch to time t; $N(t) = K \cdot \exp\{-\exp[-r(t - t_0)]\}$; all N(t = 5) cumulative-revenue values were computed analytically.

Scenario	K (MYR M)	r (yr^{-1})	t_0 (yr)	Cumulative N(t = 5) (MYR M)	Basis
Conservative	1.44	0.22	4.5	0.59	K_{base} × 0.70; slow adoption, high competition
Base	2.05	0.32	3.8	1.04	4,100 M × 0.05%; r from ASEAN analogues
Optimistic	2.67	0.42	3.2	1.67	K_{base} × 1.30; fast adoption, multi-category placement

Figures

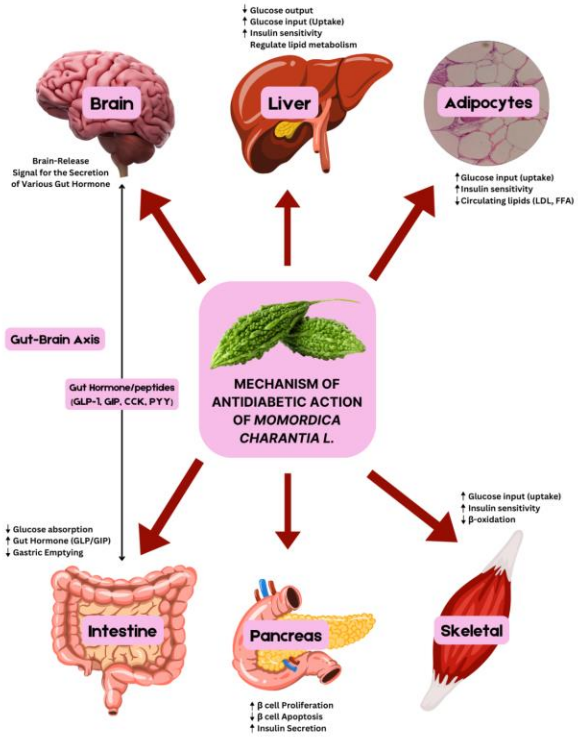

Fig. 1. Proposed multi-organ antidiabetic mechanism of *Momordica charantia* L., showing the action of its bioactive constituents on the brain, liver, adipocytes, intestine, pancreas, and skeletal muscle (adapted from (Zahoor et al., 2024)).

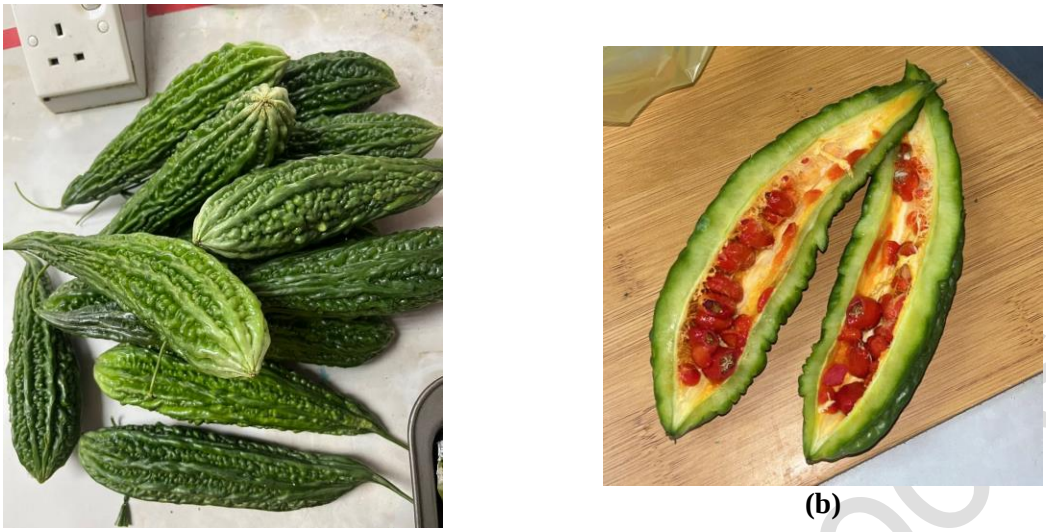

(a) **(b)**

Fig. 2. Fresh *Momordica charantia* L. raw material: **(a)** intact mature fruits as procured; **(b)** longitudinal section showing the red-arillate seed mass and the inner pulp cavity from which the bioactive-rich pulp is recovered after deseeding.

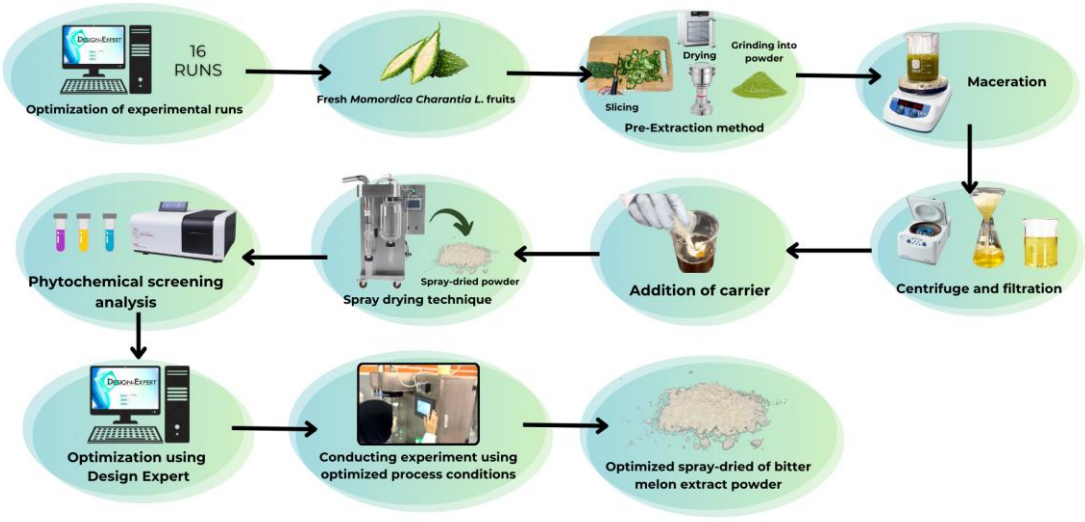

Fig. 3. Overall procedural workflow for the extraction and spray-drying microencapsulation of *M. charantia* fruit extract, comprising (in sequence): RSM two-level full factorial design (2^4) of 16 experimental runs, pre-extraction (slicing, drying, grinding) of fresh fruit, aqueous maceration, centrifugation and filtration,

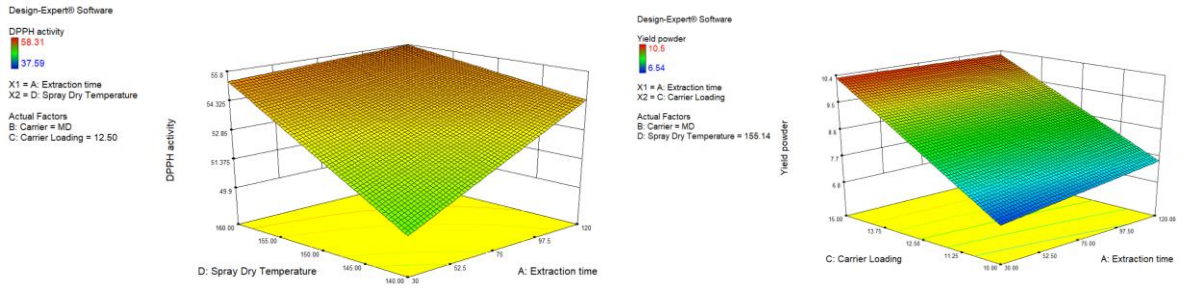

(a) **(b)**

Fig. 4. Three-dimensional response surfaces for **(a)** DPPH scavenging activity as a function of extraction time and inlet spray-drying temperature (carrier loading fixed at 12.5%; maltodextrin) and **(b)** powder yield as a function of carrier loading and extraction time (inlet temperature fixed at 155.14 °C; maltodextrin). The DPPH surface is maximised at long extraction time and low inlet temperature; the yield surface is dominated by carrier loading.

(a) **(b)**

Fig. 5. Visual appearance of the spray-dried *M. charantia* encapsulate: **(a)** optimised encapsulate produced at the desirability-function optimum (117.67 min, 15% maltodextrin, 140 °C), shown as a free-flowing off-white powder; **(b)** side-by-side comparison of the optimised encapsulate (left) and a representative non-optimised batch (right; 30 min, 10% gum arabic, 160 °C), illustrating the colour darkening and particle coarsening associated with sub-optimal carrier loading and elevated inlet temperature.

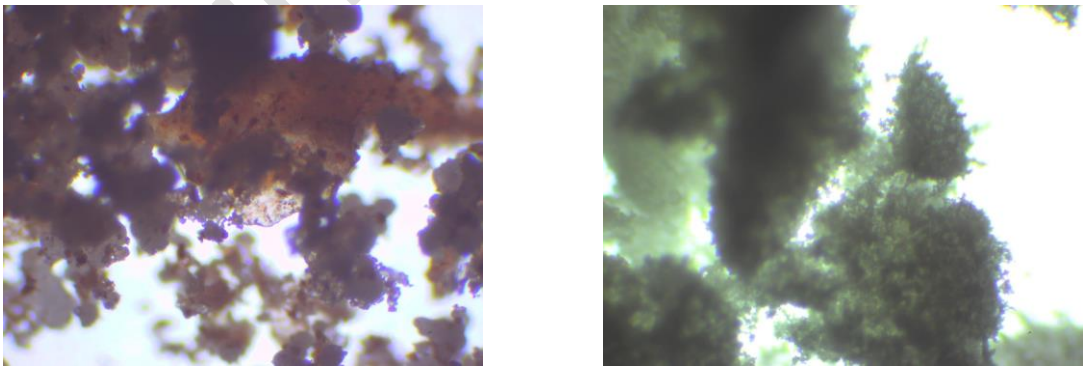

(a) **(b)**

Fig. 6. Optical microscopy (×400) of spray-dried *M. charantia* encapsulate: **(a)** non-optimised powder produced under 160 °C, 10% gum arabic, 30 min extraction, exhibiting irregular agglomerated particles with rough, folded surfaces consistent with high-Péclet-number droplet drying; **(b)** optimised powder produced at the desirability-function optimum (140 °C, 15% maltodextrin, 117.67 min extraction),

exhibiting near-spherical particles with smoother surfaces consistent with a cohesive maltodextrin shell and a reduced surface-to-core drying gradient.

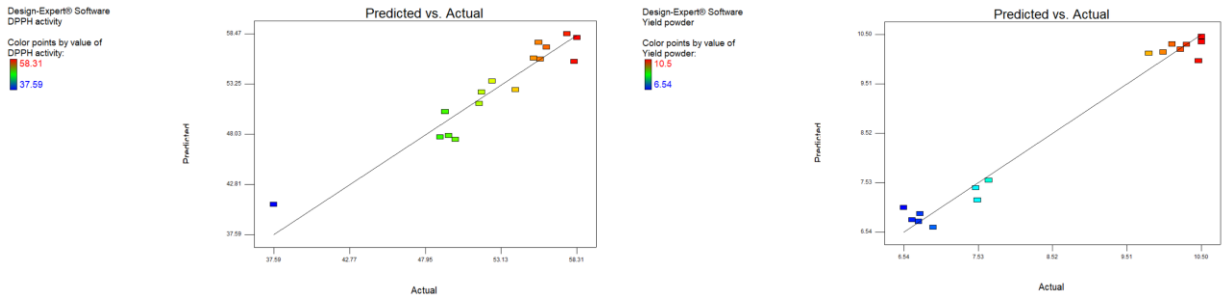

(a) **(b)**

Fig. 7. Predicted-vs.-Actual diagnostic plots of the fitted RSM models for **(a)** DPPH radical scavenging activity (visible scatter at intermediate values and a low-end outlier corresponding to Run 1; predicted R^2 = 0.0489) and **(b)** powder yield (tight clustering along the parity line across the full response range; predicted R^2 = 0.8882). Colour scale: blue = low response value, red = high response value.